Swing Contracts with Dynamic Reserves for Flexible Service Management

Shanshan Ma, *Student Member, IEEE,* Zhaoyu Wang, *Member, IEEE,* Leigh Tesfatsion, *Member, IEEE*

***Abstract*—The increasing penetration of variable energy resources in modern electric power systems requires additional flexibility in ancillary service provision to maintain reliable and efficient grid operations. However, full recognition and appropriate compensation of this flexibility is difficult to ensure within current power market designs due to rigidities in service definitions and requirements. For example, reserve requirements (RRs) are typically set in advance at administratively determined levels. If RRs are too large, wasteful expenditures result; and, if RRs are too small, high real-time costs are incurred for peak generation and/or load curtailment. To address these problems, this paper proposes a new mixed-integer linear programming (MILP) formulation for the optimal clearing of a day-ahead market based on swing contracts and a dynamic reserve method permitting the daily adaptive updating of reserve zones. Numerical examples based on a 5-bus test system are used to illustrate the effectiveness of the proposed new day-ahead market design.**

***Index Terms*—Day-ahead market, swing contract, dynamic reserve zones, flexible service provision, MILP optimization**

NOMENCLATURE

Sets and Indices

$\mathcal{B}$: Set of bus indices b
$\mathcal{B}(z) \subset \mathcal{B}$: Subset of buses in reserve zone z
$\mathcal{L} \subset \mathcal{B} \times \mathcal{B}$: Set of transmission line indices ℓ
$\mathcal{L}_{O(b)}$: Subset of lines ℓ originating at bus b
$\mathcal{L}_{E(b)}$: Subset of lines ℓ ending at bus b
$\mathcal{M}$: Set of indices m for market participants with dispatchable resources
$\mathcal{M}(b) \subset \mathcal{M}$: Subset of market participants with dispatchable resources at bus b
$\mathcal{M}(z) \subset \mathcal{M}$: Subset of market participants with dispatchable resources in reserve zone z
$\mathcal{S}$: Set of net load forecast scenarios s
$\mathcal{T}$: Set of time period indices $t = 1, \ldots, T$
$\mathcal{Z}$: Set of reserve zone indices z

Parameters and Functions

$A_m(t)$: Binary service offer indicator: 1 if m in time period t is within its contract service period; 0 otherwise
$B(\ell)$: Inverse of reactance $X(\ell)$ (p.u.) for line ℓ
c^a_m: Availability price (\$) requested by m for a swing contract that offers service availability
$d\%$: Reserve requirement percentage
$E(\ell)$: End bus for line ℓ
$NL_b(t)$: Net load forecast (MW) for bus b during t
$O(\ell)$: Originating bus for line ℓ
P^{max}_ℓ: Line flow limit (MW) for line ℓ
P^{min}_m: Lower power limit (MW) for m
P^{max}_m: Upper power limit (MW) for m
R^D_m: Ramp-down limit (MW/Δt) for m
R^U_m: Ramp-up limit (MW/Δt) for m
S_o: Positive base power (in three-phase MVA)
Δt: Time-period length
Λ_1: Imbalance penalty (\$/MW) for excess power supply
Λ_2: Imbalance penalty (\$/MW) for a power supply deficit
$\phi_m(t)$: Energy price (\$/MWΔt) as a simple form of performance payment method for real-time service offered in a swing contract

ISO Control Variables for SC DAM Optimization

$p_m(t)$: Power output (MW) of m in time period t
x_m: Binary cleared contract indicator: 1 if the swing contract offered by m is cleared; 0 otherwise
$\theta_b(t)$: Voltage angle (radians) at bus b in time period t

Solution Values Derived from SC DAM Optimization

$\overline{p}_m(t)$: Max available power output (MW) of m during t
$\underline{p}_m(t)$: Min available power output (MW) of m during t
$P_\ell(t)$: Line power (MW) for line ℓ during t
$RR^L_z(t)$: Lower spinning reserve requirement (MW) at reserve zone z during t
$RR^U_z(t)$: Upper spinning reserve requirement (MW) at reserve zone z during t
$v_m(t)$: Binary unit commitment indicator derived from x_m and $A_m(t)$: 1 if m is online in time period t; 0 otherwise
$\alpha^+_b(t)$: Non-negative slack variable indicating excess power supply (MW) at bus b during t
$\alpha^-_b(t)$: Non-negative slack variable indicating a power supply deficit (MW) at bus b during t

Last Revised 9/2/2017. This work has been supported in part by U.S. Department of Energy Office of Electricity Delivery and Energy Reliability under DE-OE 0000839. S. Ma and Z. Wang (sma@iastate.edu, wzy@iastate.edu) are with the Department of Electrical and Computer Engineering, and L. Tesfatsion (corresponding author, tesfatsi@iastate.edu) is with the Department of Economics, at Iowa State University, Ames, IA 50011.

I. INTRODUCTION

THE growing participation of variable energy resources (e.g., wind and solar power) in electric power markets has increased the importance of flexible service provision to ensure continual load-balancing capabilities [1]. This, in turn, has increased the need for a level playing field for all potential service providers that includes appropriate compensation for flexibility in service provision.

Currently, however, the appropriate compensation of service flexibility is hindered by rigid service definitions and provision requirements. For example, reserve requirements (RRs) are typically set in advance at administratively determined levels. If RRs are too large, wasteful expenditures result; and, if

RRs are too small, high real-time costs are incurred for peak generation and/or load curtailment.

In recent studies [2], [3] researchers have proposed a new swing-contract market design for electric power systems that facilitates flexible service provision. A swing contract allows a resource to offer a bundle of diverse power and ancillary services as ranges of values rather than as point values, thus permitting greater flexibility in their real-time implementation. A swing-contract market is a centrally-managed forward market that functions as a robust-control mechanism for the management of load and generation uncertainties. It permits dispatchable resources to offer services in flexible swing-contract form to ensure the availability of flexible service performance at a later date.

Subsequent studies [4]–[6] have demonstrated the practical feasibility of the swing-contract market design by developing and implementing Mixed Integer Linear Programming (MILP) formulations for the optimal clearing of swing contracts subject to standard system and reserve-requirement (RR) constraints. However, a difficulty with these optimization formulations is their reliance on exogenously specified RR levels. While service supply offers are permitted to take a flexible form, reserve demands are not. This suggests the desirability of modifying the swing-contract market design by replacing exogenously specified RR levels with some form of dynamic reserve method.

A dynamic reserve method is any process permitting the run-time adjustment of reserve demands for electric power market operations. Dynamic reserve methods currently under exploration include the adaptive updating of RR levels, reserve zones, reserve demand curves, and/or reserve deliverability status based on updated grid congestion conditions [7].

Dynamic reserve methods are particularly promising for dealing with potential power imbalances caused by high penetration of variable energy resources [8]–[12]. For example, [8] investigates whether the adaptive modification of a targeted reserve capacity over time based on expected system conditions can avoid expensive overestimation of RR with high levels of wind power. Ref. [9] proposes a heuristic rule to define dynamic reserve requirements: the reserve should be no less than 3% of load and 5% of forecasted renewable generation.

However, recent research has stressed the need to consider more carefully the effects of variable energy resources on the ability of market operators to predict network congestion, hence power transfer capabilities, in order to guarantee real-time reserve deliverability [13], [14]. To mitigate reserve deliverability problems, current U.S. ISO/RTO-managed day-ahead markets rely on pre-specified reserve zones to ensure the distribution of reserves across the transmission grid. A reserve zone is a portion of the grid that experiences relatively infrequent internal transmission congestion.

This paper proposes a new MILP formulation for the optimal clearing of swing contracts in an ISO-managed swing-contract day-ahead market (SC DAM) with dynamic reserve determination. Reserve zones and associated zonal RR requirements are adaptively adjusted each day to facilitate the balancing of net load, i.e., load minus non-dispatchable generation.

Section II describes the reformulation of the SC DAM optimization problem in [5] to incorporate reserve zones and associated zonal reserve requirements among the problem constraints. Section III explains our new proposed method for the dynamic adjustment of reserve zones and associated zonal reserve requirements. This adjustment is accomplished by means of a weighted average of shift factor differences, which in turn is based on a line-congestion risk index.

Performance testing of our new proposed dynamic reserve method in comparison with other proposed dynamic reserve methods is reported in Section IV. This testing is undertaken for a 5-bus test system consisting of a swing-contract DAM operating over a 5-bus transmission grid. Performance is measured in terms of expected energy costs and reserve delivery reliability. It is shown that our proposed method outperforms other methods in terms of these metrics. Section V concludes.

II. A Swing-Contract Market Design with Dynamic Reserve Determination

A. An Illustrative Swing Contract

As detailed in [2]–[5], a *swing contract (SC)* is a contract that permits a resource to offer the availability of a collection of power paths with a wide range of specified services, such as start-up location, start-up time, power level, ramp-rate, duration, and volt/VAr support. For concreteness, as in [5], this study will focus on the following specific form of SC permitting a dispatchable resource to offer swing (flexibility) in power levels and ramp rates:

$$\text{SC} = [b, t_s, t_e, \mathcal{P}, \mathcal{R}, \phi] \tag{1}$$

$b =$ location where service delivery is to occur;

$t_s =$ power delivery start time;

$t_e =$ power delivery end time;

$\mathcal{P} = [P^{min},\, P^{max}] =$ range of power levels p;

$\mathcal{R} = [-R^D,\, R^U] =$ range of down/up ramp rates r;

$\phi =$ Performance payment method for real-time services.

As illustrated in Fig. 1, the location b in (1) refers to a particular bus or node of a transmission grid. The start and end times t_s and t_e denote specific calendar times expressed at the granularity of time periods of length Δt (e.g., 1h, 1Min), with $t_s < t_e$. The power interval bounds $P^{min} \leq P^{max}$ can represent pure power injections (if $0 \leq P^{min}$), pure power withdrawals or absorptions (if $P^{max} \leq 0$), or bi-directional power capabilities (if $P^{min} \leq 0 \leq P^{max}$). The down/up limits $-R^D$ and R^U for the ramp rates r (MW/Δt) are assumed to satisfy $-R^D \leq 0 \leq R^U$.

The location b, the start time t_s, and the end time t_e are all specified as single values in (1). However, the power levels p and the down/up ramp rates r are specified in swing form with associated ranges $\mathcal{P}$ and $\mathcal{R}$.

The performance payment method ϕ in (1) designates the mode of ex post compensation for actual real-time service performance. As detailed in [3], ϕ can take a wide variety of forms. For example, ϕ could specify a flat-rate price ($/MWh) for down/up power delivery together with a "power-mileage" compensation for ramping based on power-path length.

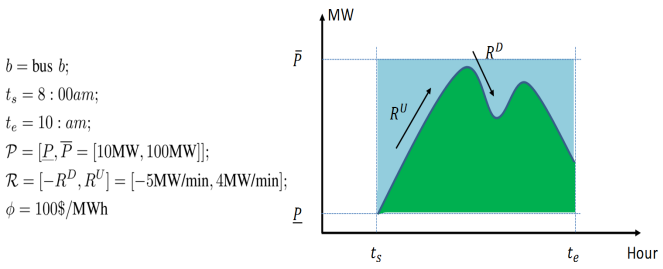

Fig. 1. (a) An illustrative swing contract with power and ramp-rate swing offered by a dispatchable resource into an ISO-managed day-ahead wholesale power market; (b) A possible power path the ISO could signal the resource to follow during next-day operations.

B. The Basic Swing-Contract Market Design

An SC market is a centrally-managed forward market that permits dispatchable resources to submit SCs offering possible real-time service performance. The SC market operator clears SC offers in advance of real-time operations in an effort to ensure the balancing of real-time net loads. To retain the market operator's non-profit status, all costs incurred by the market operator for SC procurement and use are passed through to load-serving entities in proportion to their share of serviced real-time loads.

An issuer m of a cleared swing contract SC_m is immediately paid its contract offer price c^a_m, which functions as a form of insurance premium to ensure real-time service availability. If m is subsequently dispatched to perform real-time services in accordance with SC_m, compensation is paid to m for these services in accordance with the performance payment method ϕ_m that m has included among the terms of SC_m.

It is the responsibility of issuer m to guarantee the physical and financial feasibility of its offered swing contract SC_m. With regard to physical feasibility, m must ensure it is able to fulfill the terms of SC_m, if cleared. With regard to financial feasibility, m should make sure that its contract offer price c^a_m is sufficient to cover all of the avoidable fixed costs (e.g., start-up and no-load costs) that m would incur to guarantee service *availability* in accordance with SC_m. In addition, m should make sure that its performance payment method ϕ_m is sufficient to cover all avoidable operational costs (e.g., fuel costs) that m would incur if called upon to provide real-time service *performance* in accordance with SC_m.

C. SC DAM Optimization Formulation with Dynamic Reserve

Current U.S. ISO/RTO-managed DAMs use two optimizations to determine unit commitment, generation dispatch, and pricing solutions: namely, Security-Constrained Unit Commitment (SCUC) and Security-Constrained Economic Dispatch (SCED) [15]. SCUC is formulated as a mixed integer linear programming (MILP) problem, and SCED is typically formulated as a linear programming problem.

In contrast, a single MILP optimization process is used for the ISO-managed SC DAM in [5] to determine which SCs are cleared, hence which dispatchable market participants are obligated (committed) to ensure service availability for the following day. However, this optimization process assumes pre-specified system-wide down/up spinning reserve requirements without consideration of reserve deliverability.

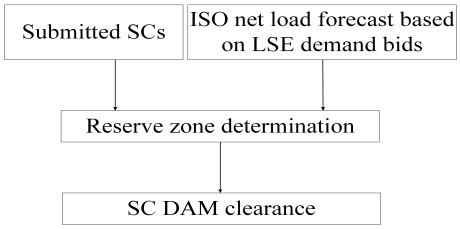

Fig. 2. Market clearing procedure for the reformulated SC DAM

In this paper we reformulate the SC DAM optimization problem developed in [5] to include the adaptive updating of reserve zones for spinning reserve. The goal of this reformulation is to achieve an SC DAM design that further reduces expected costs by improving reserve delivery reliability.

The reformulated SC DAM optimization is depicted in Fig 2. In the remainder of this section we explain this reformulated optimization for an arbitrary day D, taking as given a particular reserve zone specification. Note that the lower/upper zonal reserve requirements $RR^L_z(t)$ and $RR^U_z(t)$ associated with each reserve zone z in each time period t that appear in this reformulated optimization are endogenously determined as part of the optimal solution; hence, they depend on net load forecasts and other current system conditions. Our proposed procedure for undertaking the daily adaptive updating of the reserve zones z will be carefully explained in Section III.

Following [5, Section 5.2], eight simplifying assumptions are made for clarity of exposition. First, the SC DAM takes place on day D in order to plan for net load balancing on day D+1. Second, the 24-hours of day D+1 are represented by $\mathcal{T} = \{1, \ldots, 24\}$ with Δt = 1h. Third, all loads are fixed (must-serve) loads that do not provide dispatchable services. Fourth, all loads are serviced by Load-Serving Entities (LSEs). Fifth, an LSE's demand bid at any bus b for any hour t consists of a price-insensitive power demand (MW) reflecting the LSE's load forecast at that bus for that hour. Sixth, each market participant m with dispatchable resources offers a single swing contract SC_m into the SC DAM, where SC_m takes form (1). Seventh, the performance payment method ϕ_m appearing within SC_m takes the form of a collection of flat-rate energy prices $\phi_m(t)$ ($/MW$\Delta t$), one price for each hour $t \in \mathcal{T}$. Eighth, only spinning reserve requirements for normal load balancing purposes are considered.

Given these assumptions, the objective of the ISO managing the day-D SC DAM is to minimize total cost ($) over $\mathcal{T}$ by appropriate selection of the ISO control variables listed in the Nomenclature, subject to system and zonal reserve requirement constraints.

1) Total cost minimization objective:

$$\begin{aligned}\min \sum_{m\in\mathcal{M}} c^a_m x_m + \sum_{t\in\mathcal{T}}\sum_{m\in\mathcal{M}} \phi_m(t)\,|p_m(t)|\,\Delta t \\ +\Lambda_1 \sum_{b\in\mathcal{B}}\sum_{t\in\mathcal{T}} \alpha^+_b(t) + \Lambda_2 \sum_{b\in\mathcal{B}}\sum_{t\in\mathcal{T}} \alpha^-_b(t)\end{aligned} \tag{2}$$

Total cost is the summation of SC availability cost, expected

performance cost, and imbalance penalty cost. The latter cost proxies the additional cost that would be incurred for peak generation purchase and/or load curtailment if the SC DAM dispatch schedule is unable to ensure real-time balance between power supplies and power demands (loads).

2) Unit commitment constraints:

$$v_m(t) = x_m A_m(t),\ \forall m \in \mathcal{M}, t \in \mathcal{T} \tag{3}$$

The unit commitment $v_m(t) \in \{0,1\}$ for each market participant $m \in \mathcal{M}$ for each hour t of day D+1 is determined by two variables: the cleared contract indicator $x_m \in \{0,1\}$; and the service offer indicator $A_m(t) \in \{0,1\}$. The indicator $A_m(t)$ is a derived value, calculated by the ISO from the information provided within SC_m. For example, suppose SC_m specifies that services can be provided by m during the time interval $[t_s, t_e]$ = [10, 19] on day D+1. Then $A_m(t) = 1$ if $t \in \{10, \ldots, 19\}$ and $A_m(t) = 0$ if $t \in \{1, \ldots, 9, 20, \ldots, 24\}$. Participant m is committed to be available for service provision during hour t of day D+1 if and only if both x_m and $A_m(t)$ in (3) equal 1.

3) Voltage angle limits:

$$\theta_r(t) = 0, \forall t \in \mathcal{T} \tag{4}$$

$$-\pi \leqslant \theta_b(t) \leqslant \pi, \forall b \in \mathcal{B}, t \in \mathcal{T} \tag{5}$$

Constraints (4) determine the voltage angle specification at a designated angle reference bus r for all hours t, and constraints (5) impose voltage angle limits at all buses for all hours t.

4) Line power transmission constraints:

$$P_\ell(t) = S_0 B(l)\left[\theta_{O(\ell)}(t) - \theta_{E(\ell)}(t)\right],\ \forall \ell \in \mathcal{L}, t \in \mathcal{T} \tag{6}$$

$$-P_\ell^{max} \leqslant P_\ell(t) \leqslant P_\ell^{max},\ \forall \ell \in \mathcal{L}, t \in \mathcal{T} \tag{7}$$

5) Power balance constraints at each bus:

$$\sum_{m \in \mathcal{M}(b)} p_m(t) + \sum_{\ell \in \mathcal{L}_{E(b)}} P_\ell(t) = NL_b(t) + \sum_{\ell \in \mathcal{L}_{O(b)}} P_\ell(t) + \alpha_b^+(t) - \alpha_b^-(t),\ \forall b \in \mathcal{B}, t \in \mathcal{T} \tag{8}$$

6) Market participant capacity constraints:

$$\underline{p}_m(t) \leqslant p_m(t) \leqslant \overline{p}_m(t),\ \forall m \in \mathcal{M}, t \in \mathcal{T} \tag{9}$$

$$\overline{p}_m(t) \leqslant P_m^{max} v_m(t),\ \forall m \in \mathcal{M}, t \in \mathcal{T} \tag{10}$$

$$\underline{p}_m(t) \geqslant P_m^{min} v_m(t),\ \forall m \in \mathcal{M}, t \in \mathcal{T} \tag{11}$$

7) Market participant ramp-up and ramp-down constraints:

$$\overline{p}_m(t) - p_m(t-1) \leqslant R_m^U \Delta t v_m(t-1) + P_m^{max}[1 - v_m(t-1)],\ \forall m \in \mathcal{M}, t = 2, \ldots T \tag{12}$$

$$p_m(t-1) - \underline{p}_m(t-1) \leqslant R_m^D \Delta t v_m(t) + P_m^{max}[1 - v_m(t)],\ \forall m \in \mathcal{M}, t = 2, \ldots T \tag{13}$$

8) Zonal reserve requirement constraints:

$$\sum_{m \in \mathcal{M}(z)} \left[\overline{p}_m(t) - p_m(t)\right] \geqslant RR_z^U(t), \forall t \in \mathcal{T}, z \in \mathcal{Z} \tag{14}$$

$$\sum_{m \in \mathcal{M}(z)} \left[p_m(t) - \underline{p}_m(t)\right] \geqslant RR_z^L(t), \forall t \in \mathcal{T}, z \in \mathcal{Z} \tag{15}$$

$$\sum_{m \in \mathcal{M}} \overline{p}_m(t) \geqslant \sum_{b \in \mathcal{B}} NL_b(t) + \sum_{z \in \mathcal{Z}} RR_z^U(t), \forall t \in \mathcal{T} \tag{16}$$

$$\sum_{m \in \mathcal{M}} \underline{p}_m(t) \leqslant \sum_{b \in \mathcal{B}} NL_b(t) - \sum_{z \in \mathcal{Z}} RR_z^L(t), \forall t \in \mathcal{T} \tag{17}$$

$$RR_z^U(t) \ \geqslant\ d\% \cdot \sum_{b \in \mathcal{B}(z)} NL_b(t), \forall t \in \mathcal{T}, z \in \mathcal{Z} \tag{18}$$

$$RR_z^L(t) \ \geqslant\ d\% \cdot \sum_{b \in \mathcal{B}(z)} NL_b(t), \forall t \in \mathcal{T}, z \in \mathcal{Z} \tag{19}$$

Constraints (14)-(15) represent each reserve zone's upper and lower RR constraints for each hour t. Constraints (16)-(17) represent system-wide RR constraints for each hour t. Constraints (18)-(19) provide dynamic reserve requirements for different reserve zones: the upper and lower reserve requirements for a reserve zone z should be no less than $d\%$ of the summation of forecasted net load for that zone.

As in [5], the system inherent reserve range for hour t can be calculated as a function of the solution for the SC DAM optimization: $SIRR(t) = [RR^{min}, RR^{max}(t)]$, where

$$RR^{max}(t) = \sum_{m \in \mathcal{M}} \overline{p}_m(t),\ \forall t \in \mathcal{T} \tag{20}$$

$$RR^{min}(t) = \sum_{m \in \mathcal{M}} \underline{p}_m(t),\ \forall t \in \mathcal{T} \tag{21}$$

III. Dynamic Reserve Zone Updating Method

A. Overview

One promising approach for improving reserve delivery reliability is the adaptive updating of reserve zones based on system conditions, including net load uncertainties. Previous researchers have proposed various metrics for this purpose, such as electrical distance (ED) [16], power transfer distribution factors (PTDFs) [17], and weighted averages of PTDF differences [13].

The ED metric cannot be used to determine reserve zones for the SC DAM optimization proposed in Section II-C since voltage magnitudes for this optimization are assumed to be 1(p.u.). Also, a PTDF is a "what if" construction that does not reflect actual system conditions, especially line congestion.[1]

Perhaps for these reasons, ref. [13] instead proposes a dynamic reserve zone specification method involving the use of a weighted average of PTDF differences, where the weights are adaptively updated to reflect current system conditions. However, since this method is formulated for a standard AC optimal power flow optimization, it cannot be directly applied to our SC DAM optimization.

In this section we propose a modified version of the dynamic reserve method developed in [13] that can be used to generate daily updated reserve zone specifications for the SC DAM. Our method differs from [13] in two principle respects: (i) use of a different similarity metric (based on a line congestion risk index) to measure the similarity of buses and bus subsets; and (ii) use of a hierarchical clustering method instead of a k-mean

[1] A power transfer distribution factor PTDF$(\ell, \Delta p, b_s, b_k)$ measures the change in power flow on a power line ℓ resulting from a power increment Δp injected at a source bus b_s and withdrawn at a sink bus b_k [18].

algorithm to partition the set of grid buses into reserve zones based on bus and bus-subset similarity.

More precisely, our proposed dynamic reserve method consists of four steps to be carried out immediately prior to the operation of the SC DAM on the morning of each day D. These four steps are as follows:

Step 1: Use Monte Carlo simulations to construct a set of net load forecast scenarios;

Step 2: Use off-line preliminary optimizations to determine power line dual variable solutions, and use these solutions to construct line congestion risk indices;

Step 3: Use these indices to construct a matrix WA whose components consist of weighted averages of shift factor[2] differences;

Step 4: Use a hierarchical clustering algorithm based on WA to partition the set of buses into reserve zones for use in the day-D SC DAM.

These four steps will now be more carefully explained.

B. Construction of Net Load Forecast Scenarios

Net load is load minus non-dispatchable generation. This section explains our method for generating a set $\mathcal{S}$ of net load forecast scenarios. Each scenario takes the form $s = \{NL_b(t) \mid b \in \mathcal{B}, t \in \mathcal{T}\}$, where the terms $NL_b(t)$ are the net load forecasts appearing in our SC DAM optimization formulation in Section II-C.

For concreteness, we assume all non-dispatchable generation consists entirely of wind power. The net load forecasts $NL_b(t)$ can thus be represented as follows:

$$NL_b(t) = \hat{p}_b^L(t) - \hat{p}_b^W(t),\ \forall b \in \mathcal{B}, t \in \mathcal{T}\,, \tag{22}$$

where $\hat{p}_b^L(t)$ denotes LSE forecasted load (if any) at bus b for hour t and $\hat{p}_b^W(t)$ denotes the ISO's forecasted wind power generation (if any) at bus b for hour t.

We also assume the load forecast error $e_b^L(t)$ and the wind power generation forecast error $e_b^W(t)$ are uncorrelated random variables governed by mean-zero normal distributions for each $b \in \mathcal{B}$ and $t \in \mathcal{T}$. The standard deviations for the net load forecast errors can thus be expressed as:

$$\sigma_b^{NL}(t) = \sqrt{\sigma_b^L(t)^2 + \sigma_b^W(t)^2},\ \forall b \in \mathcal{B}, t \in \mathcal{T}\,. \tag{23}$$

In (23), $\sigma_b^L(t)$ denotes the standard deviation of the load forecast error $e_b^L(t)$ and $\sigma_b^W(t)$ denotes the standard deviation of the wind power generation forecast error $e_b^W(t)$. Hence, the net load forecast $NL_b(t)$ has a mean-zero normally-distributed forecast error $e_b^{NL}(t)$ with standard deviation $\sigma_b^{NL}(t)$ [19].

We then use Monte Carlo simulation to generate multiple net load forecast scenarios s as perturbations about a base net load scenario taken to represent true expected net load.

C. Line Congestion Risk Index Calculation

Transmission lines that are frequently congested are generally referred to as *critical* lines. In the SC DAM optimization formulation developed in Section II-C, the dual variables ("shadow prices") corresponding to the lower and upper inequality constraints in (7) for line power flows indicate the congestion status of the transmission lines. In this section we explain how the solution values for these dual variables can be used to construct a "line congestion risk index" for each line $\ell \in \mathcal{L}$ that indicates the degree to which line ℓ is critical.

First, we construct a set $\mathcal{S}$ of net load forecast scenarios s using the method described in Section III-B. Second, for each scenario $s \in \mathcal{S}$, we solve the SC DAM optimization problem in Section II-C assuming the set $\mathcal{B}$ of all grid buses constitutes a single reserve zone. Third, we record the resulting 0-1 unit commitment solution values $v_m^s(t)$. Fourth, we re-solve the SC DAM optimization problem for each scenario $s \in \mathcal{S}$, taking as given the unit commitment solution values $v_m^s(t)$. Finally, we record the resulting dual variable solution values $\lambda_{\ell,s}^1(t)$ and $\lambda_{\ell,s}^2(t)$ corresponding to the lower and upper line power inequality constraints in (7).

The *line congestion risk index* for each line $\ell \in \mathcal{L}$ is then calculated as follows:

$$w_\ell = \frac{\sum_{s\in\mathcal{S}} \sum_{t\in\mathcal{T}} \max\left\{|\lambda_{\ell,s}^1(t)|, |\lambda_{\ell,s}^2(t)|\right\}}{|\mathcal{T}| \cdot |\mathcal{S}|}\,. \tag{24}$$

By construction, the larger the value of w_ℓ, the more likely it is that line ℓ will experience congestion, conditional on the set $\mathcal{S}$ of net load forecast scenarios.

D. Weighted Average of Shift Factor Differences

Let $\text{SF}_{\ell,i}^r = \text{SF}(\ell, 1\text{MW}, i, b_r)$ denote the shift factor that measures the change in power flow on line ℓ when 1MW of power is injected at bus i and withdrawn at a fixed reference bus b_r; cf. footnotes 1 and 2. Given any two buses i and j, we construct a weighted average of shift factor differences for these buses as follows:

$$\text{WA}_{ij} = \frac{\sum_{\ell\in\mathcal{L}} w_l |\text{SF}_{\ell,i}^r - \text{SF}_{\ell,j}^r|}{|\mathcal{L}|}\,, \tag{25}$$

where the weights w_ℓ in (25) are the line congestion risk indices given by (24). Finally, the matrix whose components are given by $\text{WA}_{i,j}$ is denoted by WA.

E. Hierarchical Clustering Method for Reserve Zone Partition

The well-known hierarchical clustering method developed by [20] proceeds as follows. Consider a finite set $\mathcal{N}$ consisting of $N \geq 2$ elements for which the dissimilarity between any two elements i and j in $\mathcal{N}$ is measured by some designated dissimilarity metric $d(i, j)$. The dissimilarity between any two disjoint subsets of $\mathcal{N}$ can then be measured in a variety of ways: e.g., via *average dissimilarity* calculated as the average dissimilarity between any element of one subset and any element of the other subset.

Start with a partition $P(N)$ of $\mathcal{N}$ into N disjoint subsets, each subset containing a single element. Find a pair of subsets in $P(N)$ whose dissimilarity to each other is at least as small as between any other two subsets in $P(N)$ and merge these two subsets; this results in a partition $P(N-1)$ of $\mathcal{N}$ into

[2] A shift factor $\text{SF}(\ell, \Delta p, b_s, b_r)$ differs from a PTDF with regard to the specification of the sink bus. For shift factors, the sink bus is always designated to be some fixed reference bus b_r [18].

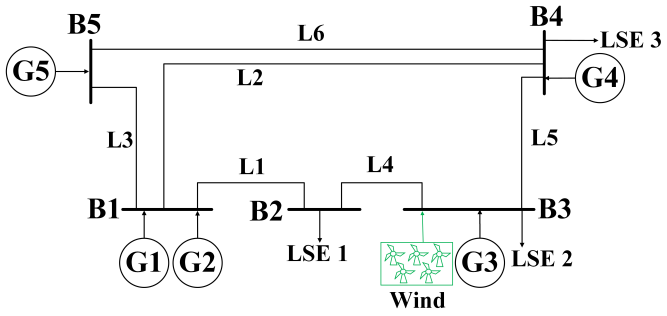

Fig. 3. Five-bus test system

$N-1$ disjoint subsets. Repeat this process until one obtains $P(1)$, a "partition" of $\mathcal{N}$ into one subset $\mathcal{N}$.

At each stage of this clustering process, by construction, the dissimilarity between the two merged subsets is non-decreasing. If the goal is to obtain a partitioning of $\mathcal{N}$ into subsets that display internal element similarity and between-subset dissimilarity, a natural place to stop the process is at a point where the dissimilarity between the next two subsets to be merged exhibits a sharp increase.

In the current study, this hierarchical clustering method is applied to the set $\mathcal{B}$ consisting of all grid buses in order to partition $\mathcal{B}$ into reserve zones. The dissimilarity between any two buses i and j in $\mathcal{B}$ is measured by $\text{WA}_{i,j}$, and the dissimilarity between any two disjoint bus subsets is measured by the average dissimilarity of their bus elements. A sharp increase in subset dissimilarity is used to determine the point at which the clustering process is halted.

IV. Comparative Performance Simulation Study

A. Overview

This section reports findings from a simulation study undertaken to test the ability of dynamic reserve methods to enhance the performance of the basic swing-contract day-ahead market (SC DAM) design presented in Section II. Three different methods for adaptive reserve-zone updating are considered: the PTDF method proposed in [17]; the weighted PTDF difference method proposed in [13]; and our modified version of [13], presented in Section III, that makes use of line congestion risk indices and hierarchical clustering.

The five-bus test system used for this study, adapted from [21], is depicted in Fig. 3. The grid consists of five buses B1-B5 and six transmission lines L1-L6. The participants include: five dispatchable thermal generation units G1-G5 located at buses B1, B3, B4, and B5; one non-dispatchable wind farm located at bus B3; and three LSEs servicing load at buses B2, B3, and B4. The designated reference bus is B4.

All simulations were carried out on the Iowa State University Condo cluster, whose individual blades consist of two 2.6 GHz 8-Core Intel E5-2640 v3 processors and 128GB of RAM. Pyomo 5.3.0 was used to formulate and solve the SC DAM optimization problem; CPLEX Python API 12.6 was employed as the MILP solver.

B. Configuration of the Five-Bus Test System

The time step for the SC DAM was set at Δt = 1h, and the planning horizon $\mathcal{T}$ was specified to be 24 hours. The reserve requirement percentage $d\%$ was set at 5%. The imbalance penalties for excess and deficit power were set at Λ_1 = 1000\$/MW and Λ_2 = 1000\$/MW. The positive base power S_o was set equal to 100 MVA. The physical characteristics of the six transmission lines are given in Table I.

TABLE I
Transmission Line Data

Line	From Bus	To Bus	X(p.u.)	Flow Limit(MW)
L1	B1	B2	0.0281	350
L2	B1	B4	0.0304	300
L3	B1	B5	0.0064	250
L4	B2	B3	0.0108	200
L5	B3	B4	0.0297	150
L6	B4	B5	0.0297	240

Wind power at bus B3 was simulated as a normally distributed power output with a standard deviation of 10% from expected value. Hourly load was simulated as a normally distributed power demand with a standard deviation of 2% from expected value. Simulated hourly load was distributed across buses B2, B3, and B4 as 40%, 30%, and 30% of total load, respectively.

The Monte Carlo procedure explained in Section III-B was used to construct a set $\mathcal{S}$ consisting of 1000 net load forecast scenarios s, each 24 hours in length, for the five-bus test system. The net load at a particular bus during a particular hour equals load (if any) minus non-dispatchable wind power generation (if any). For the five-bus test system, net load is always zero at B1 and B5 since only thermal generation is present. Consequently, each scenario $s \in \mathcal{S}$ designates net load forecasts only for buses B2, B3, and B4. An illustrative scenario is depicted in Fig. 4.

The swing contracts submitted into the SC DAM by G1-G5 all take form (1); hence, swing (flexibility) is offered in power and ramp-rate levels. These swing contracts are shown in Table II.

For our dynamic reserve-zone updating method proposed in Section III, the bus dissimilarity matrix WA with components (25) was calculated to be

$$\text{WA} = \begin{Bmatrix} 0 & 0.1837 & 0.2543 & 0.4457 & 1.0720 \\ 0.1837 & 0 & 0.0706 & 0.2650 & 0.8914 \\ 0.2543 & 0.0706 & 0 & 0.1955 & 0.8219 \\ 0.4457 & 0.2650 & 0.1955 & 0 & 0.6278 \\ 1.0720 & 0.8914 & 0.8219 & 0.6278 & 0 \end{Bmatrix} \tag{26}$$

Hierarchical clustering based on WA was then used to partition the set of five buses into two reserve zones, as shown in Fig. 5.

TABLE II
SWING CONTRACTS (SCS) SUBMITTED BY THE FIVE SC DAM PARTICIPANTS WITH DISPATCHABLE GENERATION

Thermal Gen Units	Service Period $[t_e, t_s]$	Power Range $[P^{min}, P^{max}]$(MW)	Ramp Rate Range $[-R^D, R^U]$(MW/h)	Available Price $c^a(\$)$	Performance Price $\phi(\$/\text{MWh})$
G1	$[5, 24]$	$[10, 110]$	$[-32, 32]$	1500	14
G2	$[1, 20]$	$[10, 100]$	$[-50, 50]$	1700	15
G3	$[1, 24]$	$[50, 520]$	$[-104, 104]$	2000	25
G4	$[4, 20]$	$[20, 200]$	$[-60, 60]$	1800	30
G5	$[1, 24]$	$[40, 600]$	$[-120, 120]$	1600	10

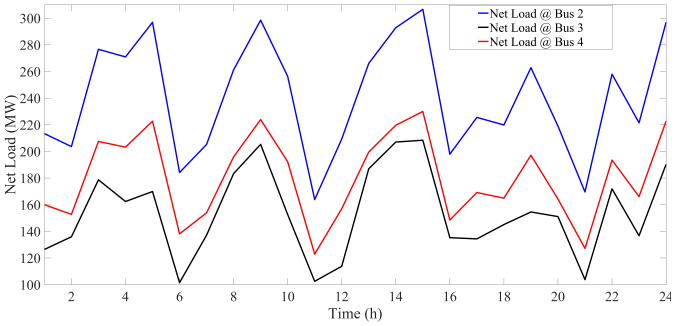

Hour	1	2	3	4	5	6	7	8	9	10	11	12
NL_2	213	203	276	270	296	184	205	261	298	256	163	209
NL_3	126	136	179	162	170	101	137	183	205	153	102	114
NL_4	160	153	207	203	223	138	154	196	224	192	123	157
Hour	13	14	15	16	17	18	19	20	21	22	23	24
NL_2	266	293	307	198	225	220	262	219	170	258	221	297
NL_3	187	207	208	135	134	145	155	151	104	172	137	190
NL_4	200	220	230	148	169	165	197	164	127	193	166	223

Fig. 4. An illustrative net load forecast scenario for the five-bus test system.

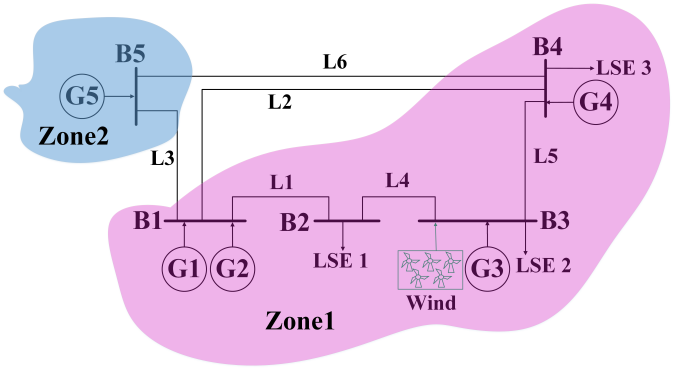

Fig. 5. Reserve zones for the five-bus test system as determined by hierarchical clustering.

C. Key Findings

Expected cost outcomes were calculated for the SC DAM operating under three different methods for the adaptive updating of reserve zones: namely, the PTDF method proposed in [17]; the weighted PTDF difference method proposed in [13]; and our new dynamic reserve method proposed in Section III. As explained with care in Section II-C, expected cost for the

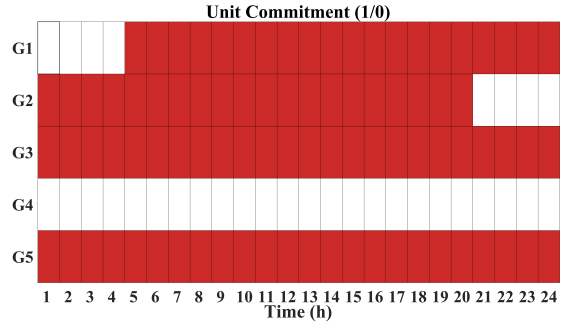

Fig. 6. The unit commitment determined by the SC DAM optimization using our proposed new dynamic reserve method

SC DAM is the summation availability cost, performance cost, and penalty cost for power supply excesses or deficits in real-time operations.

Expected cost comparisons are presented in Table III. These comparisons indicate that our new dynamic reserve method results in the lowest expected cost.

TABLE III
EXPECTED COST UNDER THREE DIFFERENT DYNAMIC RESERVE METHODS

Method	Reserve Zones	Cleared SCs	Expected Cost
[17]	Z1:Bus 2, 3, 4	G1 G2	$\$187,877.68$
	Z2:Bus1, 5	G3 G5	
[13]	Z1:Bus 2, 3	G1 G2	$\$186,113.18$
	Z2:Bus 1, 5	G3 G5	
Our	Z1: Bus 1 2, 3, 4	G1 G2	$\$183,611.70$
method	Z2: Bus 5	G3 G5	

Under our method, the SC DAM optimization solution clears the SCs submitted by G1, G2, G3, and G5; however, the SC submitted by G4 is not cleared. The only information communicated by the ISO back to G1-G5 is their unit commitment status, i.e., whether or not their SC was cleared. However, the SC DAM optimization solution also results in a dispatch schedule for next-day operations that the ISO can use as a planning device. The unit commitment and dispatch schedule, shown in Fig. 6 and Fig. 7, respectively, reveal that the ISO anticipates using G5 as a base-load unit due to its relatively low performance cost.

Figure 8 reports additional information about the SC DAM

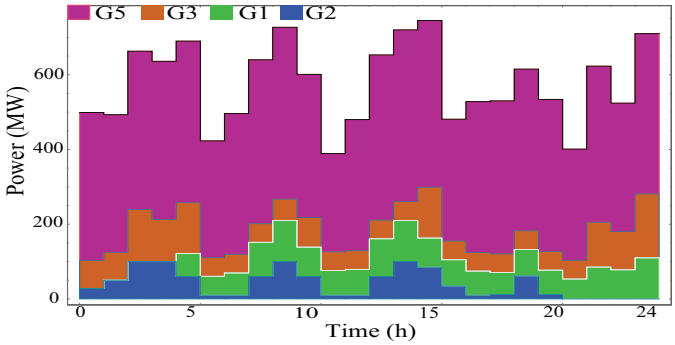

Fig. 7. The power dispatch schedule determined by the SC DAM optimization using our proposed new dynamic reserve method.

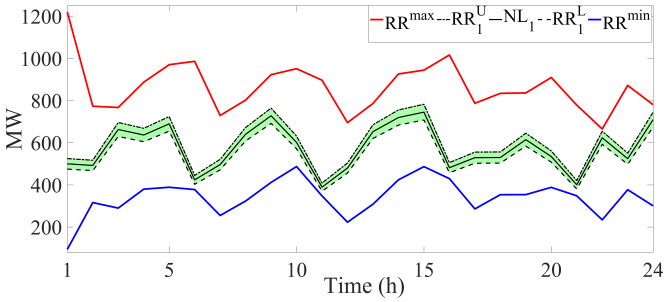

Fig. 8. Dynamically determined reserve ranges relative to forecasted net load in Reserve Zone 1 under our proposed new dynamic reserve method.

optimization solution resulting under our method. By construction, only Reserve Zone 1 has non-zero forecasted net load. Fig. 8 depicts this forecasted net load together with the lower and upper zonal reserve requirements $RR_1^L(t)$ and $RR_1^U(t)$ determined endogenously for Reserve Zone 1 along the SC DAM optimization solution path. Also superimposed in Fig. 8 is the endogenously determined system inherent reserve range *SIRR* with lower and upper range limits given by $RR^{min}(t)$ and $RR^{max}(t)$ for each hour t. *SIRR* is a run-time reserve measure that encompasses reserve from all zones; see Section II for a detailed explanation of the *SIRR*.

As seen in Fig. 8, zonal forecasted net load is well covered by the endogenously determined zonal reserve ranges resulting from the SC DAM optimization under our proposed dynamic reserve method. In particular, the width of these zonal reserve ranges is typically wider than minimally required by the $d\%$ reserve requirement percentage and varies over time in response to anticipated system conditions.

V. Conclusion

This paper proposes a swing-contract day-ahead market (SC DAM) optimization formulation that incorporates a new dynamic reserve method for the adaptive updating of reserve zones and zonal reserve requirements. The optimization formulation is expressed as a mixed integer linear programming (MILP) problem and solved using a standard MILP solver.

Comparative simulation studies are carried out for an SC DAM operating over a five-bus transmission grid to test the effectiveness of our new proposed dynamic reserve method. Expected cost outcomes indicate that our method results in lower expected costs of operation for the SC DAM than the dynamic reserve methods proposed in [17] and [13].

References

[1] E. Hsieh and R. Anderson, "Grid flexibility: The quiet revolution," *The Electricity Journal*, vol. 30, no. 2, pp. 1–8, March 2017.

[2] L. S. Tesfatsion, C. A. Silva-Monroy, V. W. Loose, J. F. Ellison, R. T. Elliott, R. H. Byrne, and R. T. Guttromson, "New wholesale power market design using linked forward markets," *Sandia National Laboratories Report (SAND2013-2789), April*, 2013.

[3] D.-Y. Heo and L. S. Tesfatsion, "Facilitating appropriate compensation of electric energy and reserve through standardized contracts with swing," *Journal of Energy Markets*, vol. 8, no. 4, pp. 93–121, December 2015.

[4] W. Li and L. Tesfatsion, "Market provision of flexible energy/reserve contracts: Optimization formulation," in *Proc. IEEE Power and Energy Society General Meeting (PESGM)*, Jul. 2016.

[5] ——, "A swing-contract market design for flexible service provision in electric power systems," in *Energy Markets and Responsive Grids: Modelling, Control, and Optimization*, S. Meyn, T. Samad, S. Glavaski, I. Kiskens, and J. Stoustrup, Eds. Springer Verlag, 2017.

[6] J. Hansen, A. Somani, Y. Sun, and Y. Zhang, "Auction design for power markets based on standardized contracts for energy and reserves," in *Proc. IEEE Power and Energy Society General Meeting (PESGM)*, Jul. 2016.

[7] K. W. Hedman, M. Zhang, and M. Ilic, "Markets for ancillary services in the presence of stochastic resources," *Final Project Report M-31, PSERC Publication 16-06*, September 2016.

[8] H. Holttinen, M. Milligan, E. Ela, N. Menemenlis, J. Dobschinski, B. Rawn, R. J. Bessa, D. Flynn, E. Gomez-Lazaro, and N. K. Detlefsen, "Methodologies to determine operating reserves due to increased wind power," *IEEE Transactions on Sustainable Energy*, vol. 3, no. 4, pp. 713–723, 2012.

[9] NREL, "Western wind and solar integration study," NREL/SR-550-47434. Golden, Colorado: National Renewable Energy Laboratory, Tech. Rep., 2010.

[10] K. De Vos and J. Driesen, "Dynamic operating reserve strategies for wind power integration," *IET Renewable Power Generation*, vol. 8, no. 6, pp. 598–610, 2014.

[11] J. Kiviluoma, P. Meibom, A. Tuohy, N. Troy, M. Milligan, B. Lange, M. Gibescu, and M. O'Malley, "Short-term energy balancing with increasing levels of wind energy," *IEEE Transactions on Sustainable Energy*, vol. 3, no. 4, pp. 769–776, 2012.

[12] N. G. Paterakis, O. Erdin, A. G. Bakirtzis, and J. P. Catalo, "Qualification and quantification of reserves in power systems under high wind generation penetration considering demand response," *IEEE Transactions on Sustainable Energy*, vol. 6, no. 1, pp. 88–103, 2015.

[13] F. Wang and K. W. Hedman, "Dynamic reserve zones for day-ahead unit commitment with renewable resources," *IEEE Transactions on Power Systems*, vol. 30, no. 2, pp. 612–620, 2015.

[14] J. D. Lyon, F. Wang, K. W. Hedman, and M. Zhang, "Market implications and pricing of dynamic reserve policies for systems with renewables," *IEEE Transactions on Power Systems*, vol. 30, no. 3, pp. 1593–1602, 2015.

[15] National Academies of Sciences, Engineering, and Medicine, "Analytic research foundations for the next-generation grid," National Academies Press, Washington, DC, Tech. Rep., 2016.

[16] E. Cotilla-Sanchez, P. D. Hines, C. Barrows, S. Blumsack, and M. Patel, "Multi-attribute partitioning of power networks based on electrical distance," *IEEE Transactions on Power Systems*, vol. 28, no. 4, pp. 4979–4987, 2013.

[17] F. Wang and K. W. Hedman, "Reserve zone determination based on statistical clustering methods," in *North American Power Symposium (NAPS)*. IEEE, 2012, pp. 1–6.

[18] E. Litvinov, "Power system and LMP fundamentals," *WEM301, ISO New England Inc.*, 2008.

[19] M. A. Matos and R. J. Bessa, "Setting the operating reserve using probabilistic wind power forecasts," *IEEE Transactions on Power Systems*, vol. 26, no. 2, pp. 594–603, 2011.

[20] S. C. Johnson, "Hierarchical clustering schemes," *Psychometrika*, vol. 32, no. 3, pp. 241–254, 1967.

[21] H. Li and L. Tesfatsion, "ISO net surplus collection and allocation in wholesale power markets under LMP," *IEEE Transactions on Power Systems*, vol. 26, no. 2, pp. 627–641, 2011.